WESTERN PACIFIC EARTH SCIENCES
Vol.1, No.1, P.73-84, 6 Figs., February, 2001

THREE-DIMENSIONAL P- AND S-WAVE VELOCITY STRUCTURES OF THE CHINGSHUI-TUCHANG GEOTHERMAL AREA IN NORTHEASTERN TAIWAN

C.H. LIN AND Y.H. YEH

Institute of Earth Sciences, Academia Sinica, Taipei, Taiwan, R.O.C.

ABSTRACT

Crustal velocity structure of the Chingshui-Tuchang area is obtained from the analysis of P- and S-wave arrivals of 257 local earthquakes recorded by a temporary seismic network in Ilan, northeastern Taiwan. The results of one-dimensional structure show that a major discontinuity in the uppercrust is found at the depth of 3 km for both P- and S-wave velocities. In addition, a significantly low S-wave velocity layer is found at depth between 10-15 km. This feature is similar to that of a partially molten magma body found in other geothermal areas, such as Yellowstone. Three-dimensional P-wave velocity structures show that lateral variations in P-wave velocity in the shallow depths are generally associated with the geological structures near the surface. The major geothermal areas such as Chingshui and Tuchang exhibit lower P-wave velocity. Relocated earthquakes using the three-dimensional model show that many of the earthquakes are located in high velocity areas or areas with large gradient in the upper crust.

Key words: seismic tomography, geothermal areas, crustal structures, seismicity, magma

INTRODUCTION

The Chingshui-Tuchang area is one of the most active geothermal areas in Taiwan. It is located to the south of the Ilan plain, which is believed to be the westward extension of the Okinawa trough (Suppe, 1984; Yeh *et al.*, 1989; Liu, 1995). Many hot springs have been found in this area, particularly at Chingshui and Tuchang. During the past decade, some geological surveys and geophysical studies have been done (e.g., Tseng, 1977; Yu *et al.*, 1977; Tsai *et al.*, 1978), but details regarding the deep structures in the crust are absent while the possible heat source of this geothermal area is not yet fully understood.

The major purpose of this study is to study the three-dimensional velocity structures in the Chingshui-Tuchang geothermal area. First, the arrivals of both P- and S-waves generated by 257 local earthquakes and recorded by a temporary seismic network are selected to invert a one-dimensional velocity model. Based on this model, a three-dimensional velocity model is then inverted. In the meantime, all of the earthquakes are relocated on the basis of the three-dimensional model. Finally, the velocity structures and relocated earthquakes are discussed in two NW-SE profiles perpendicular to the strike of the geological structures near the surface.

GEOLOGICAL SETTING AND SEISMIC DATA

The general geology and main structures in the Chingshui-Tuchang geothermal area are shown in Figure 1. This geothermal area is located to the south of the Ilan plain, which, reportedly, represents the western extension of the Okinawa trough in Taiwan (Suppe, 1984; Yeh *et al.*, 1989; Liu, 1995). Major faults in the Chingshui-Tuchang area from northwest to southeast include the Neodou, Hsiaonanao, Hanchi and Wumaoshan faults. They basically trend in the NE or NEE directions and dip to the southeast (Tseng, 1978; Ho, 1988). West of the Neudou fault, the rocks belong to the Oligocene. Rocks exposed to the east of the Wumaoshan fault belong to the Eocene and Late Paleozoic. The rocks cropping out in the Chingshui-Tuchang area between the Neodou and Wumaoshan faults belong primarily to the Lushan Formation of the Miocene age, with some scattered distribution of the Oligocene Kankou Formation, the Eocene-Oligocene Sandstone and Eocene Tungshan Formation (Tseng, 1978).

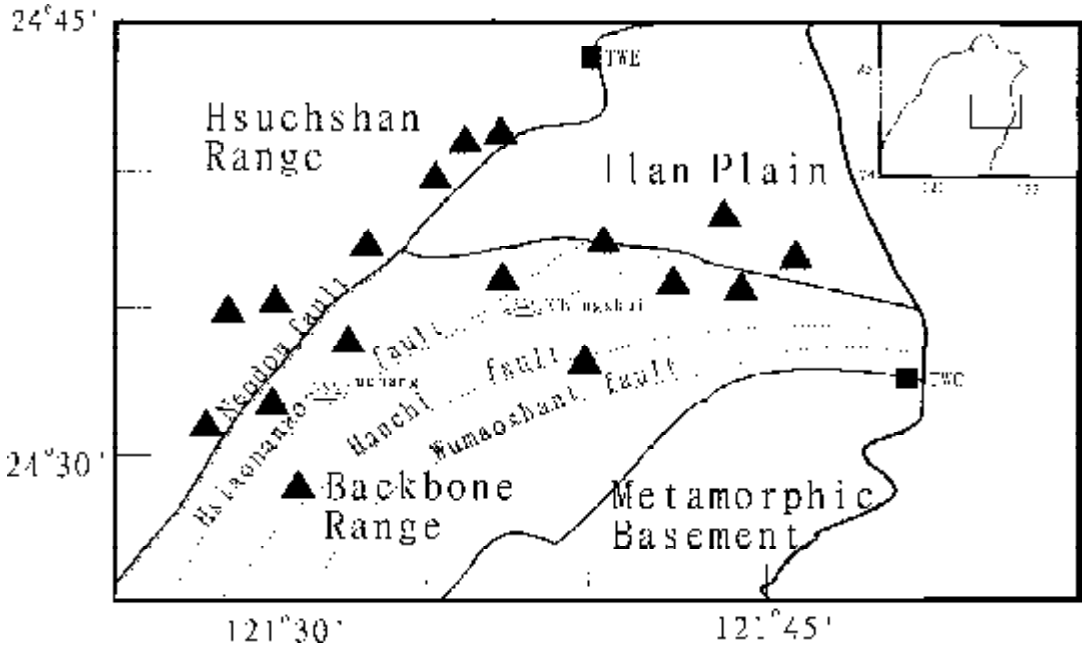

Figure 1. Locations of temporary stations (triangles) and two TTSN stations in the Chingshui-Tuchang area installed by the Institute of Earth Sciences, Academia Sinica (Yu *et al.*, 1997) and the general geology modified from Ho (1988) and Tseng (1977).

Seismic data used in this study were recorded by a temporary seismographic network in this area (Yu *et al.*, 1977). The network was installed by the Institute of Earth Sciences, Academia Sinica, for the period from Dec. 28, 1976 to Feb. 12, 1977. The network, with 13 temporary stations and two permanent stations of the Taiwan Telemetered Seismographic Network (TTSN), covers an area 40 km by 20 km (Fig. 1). During the experiment, some temporary stations were moved in order to record more earthquakes. Arrivals of P-waves as generated by 257 local earthquakes and recorded by this network are selected to invert the three-dimensional velocity structures. The error of the best time pick of the first arrival times is estimated to be 0.02 sec. Less precise picks are also included, but are given correspondingly smaller weights during inversion.

METHODOLOGY

A seismic tomography (Roecker, 1982; Roecker *et al.*, 1987) is used in this study to determine the three-dimensional velocity structures and relocate the earthquakes. During the past decade, the authors had been using this method successfully to investigate several places of tectonic interest and provide reliable three-dimensional images of the Taiwan area (Lin *et al.*, 1989; Yeh *et al.*, 1989). In this method, the velocities in a discretized model of the crust and uppermost mantle and the hypocentral parameters are determined simultaneously by minimizing the travel time residuals of P-waves from earthquakes recorded locally. The detailed inversion theory is described elsewhere (e.g. Roecker, 1982; Roecker *et al.*, 1987). Here only the inversion procedures applied in this study are briefly presented.

An iterative two-step procedure of a damped least-squares inversion is used to obtain the final structures. First, the earthquakes are located by an assumed starting one-dimensional structure or, later, by an intermediate three-dimensional structure. The one-dimensional structure is parameterized by a set of layers bound by horizontal interfaces, and the three-dimensional structure bounded by two orthogonal sets of vertical interfaces embedded in the horizontal layers. Second, the velocities of this structure are perturbed on the basis of the residuals of the travel times of the P-wave arrivals. These two steps are performed iteratively until the residual variance is more or less equal to the arrival errors.

ONE-DIMENSIONAL STRUCTURE

A suitable one-dimensional structure has to be determined as a starting model for the three-dimensional inversion. To find the optimum interface depths in the study area, we first invert structure from two multi-layer models, M1 and M2, with different depths. The layer boundaries are set at 1, 3, 5, 7, 9 11, 13, 15, 18, 22 and 26 km in model M1, and at 2, 4, 6, 8, 10, 12, 14, 16, 20, 24 and 28 km in model M2 (Fig. 2). The velocities of both models are assumed to linearly increase with depth, while the velocity ratio of P- to S-waves is assumed to be 1.78. After the iterative procedure of damped least-squares inversion, the velocity models are obtained, as shown in Figure 2. In the upper crust, the major discontinuities are found at 1 km and 3 km in model M1, and at 2 km and 4 km in model M2. Velocities do not increase abruptly around depths of 5-9 km in either model. In the mid-crust, some minor discontinuities are located at 9 km and 13 km in model M1, and 10 km and 14 km in model M2. At depths greater than 15 km, velocities increase gradually in both models.

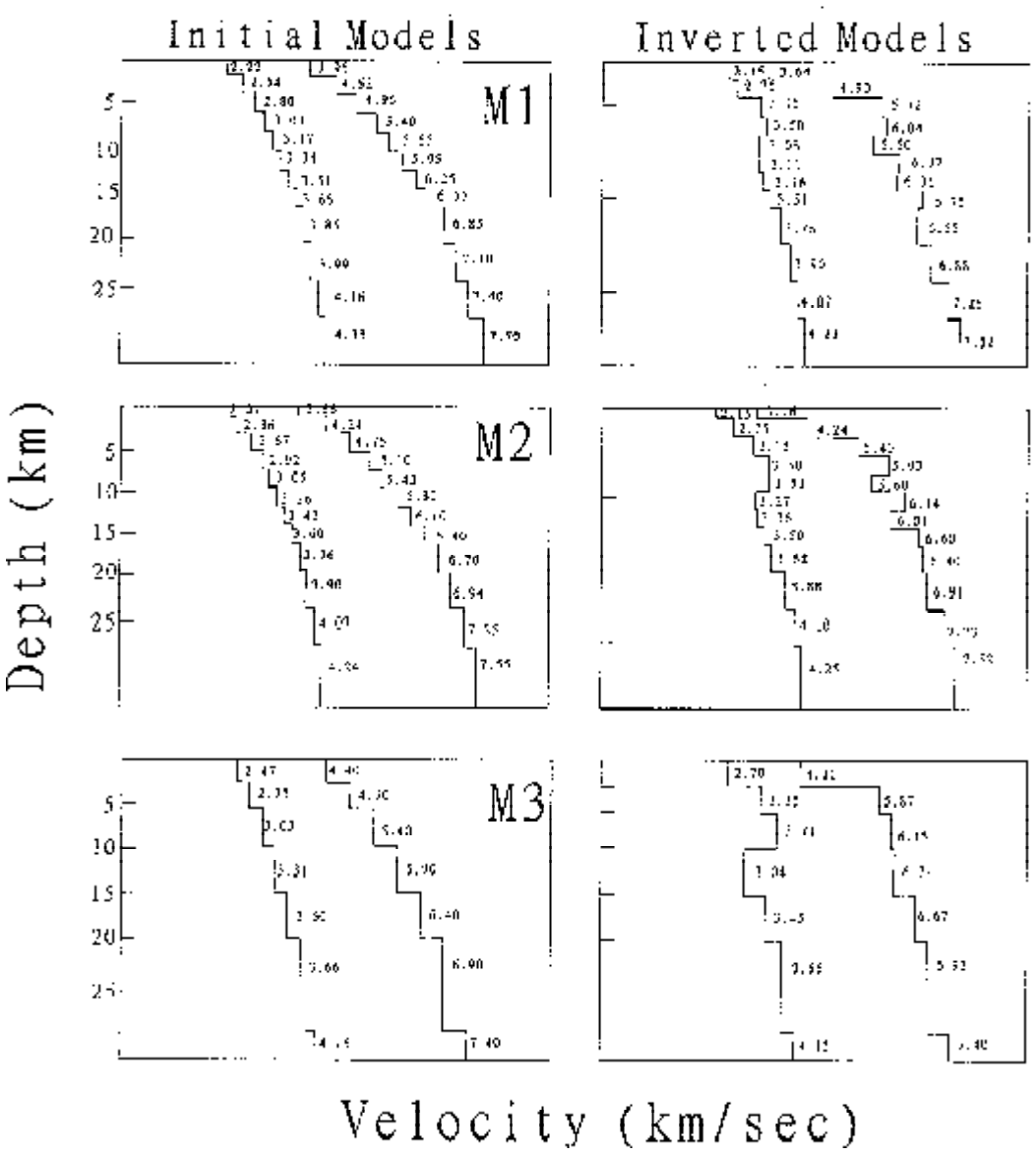

Figure 2. One-dimensional P- and S-wave models (M1, M2 and M3) before (left) and after (right) tomographic inversions. Values in models show velocity (km/sec) in each layer.

On the basis of models M1 and M2, we reconstruct a new model (M3) with 6-layers and a half-space to invert the one-dimensional model. Starting P-wave velocities are increased linearly at depths of 3, 6, 10, 15, 20 and 30 km. The velocity ratio of P- to S-waves is again assumed to be 1.78. After the iterative procedure of damped least-squares inversion, velocities of P-waves in the final model are 4.24, 5.87, 6.13, 6.21, 6.67, 6.93 and 7.40 km/sec (Fig. 2). It is interesting to note that velocity increases significantly at the depth of 3 km, which is a major discontinuity in the study area. Some other minor discontinuities in P-waves are found at the depths of 15 km and 30 km. Velocities do not change too much at depths between 6 and 15 km.

For S-wave velocities, some other features are of interest. In addition to the major discontinuity at 3 km, there is a significantly low velocity layer at depths between 10-15 km. This feature similarly found in the geothermal areas of Yellowstone National Part (Chatterjee *et al.*, 1976) and The Geysers (Majer and McEvilly, 1976) where a partially molten magma exhibits low S-wave velocity. Thus, the low S-wave velocity in the mid-crust in this study might further imply that the western opening of the Okinawa trough extends to not only the Ilan plain (Suppe, 1984; Yeh *et al.*, 1989; Liu, 1995) but also beneath the Chingshui-Tuchang area.

THREE-DIMENSIONAL STRUCTURE

The initial model of three-dimensional velocity structures is constructed from the one-dimensional velocity model, as described in the previous section. Each layer is divided into a number of rectangular prisms by two orthogonal sets of vertical interfaces to simulate a three-dimensional structure. Judging from the major strike of the surface geology, one set of the interfaces is oriented along N50^{o}E, whereas the other is in the N40^{o}W direction. The positions of the vertical interfaces in layer 1 are chosen such that each station basically occupies a separate block.

The inverted velocities in each layer are illustrated in the contour maps in Figure 3. To show the reliability of the three-dimensional structures, we only plot the contours within those blocks with inverted resolution greater than 0.5. The lower velocity area is marked with an "L", and the higher velocity area is marked with an "H".

In the first layer (0-3 km), the general pattern of the velocity structures is compatible with the surface geological features. The general trend of P-wave velocity is parallel to the strike of most faults striking in the NE-SW direction. Velocities increasing southeastward reflect the rock characteristics exposed on the surface. For example, high velocity (H1) is probably associated with the Paleogene rocks in the eastern part of the study area. Low velocity (L1), on the other hand, is related to the Neogene rocks in the southwestern part of the study area, just east of the Neodou fault.

In the second layer (3-6 km), velocity structures are more complicated than those in the first. Two local higher areas (H1 and H2) are found in the eastern and western parts of the study area, respectively. The higher velocity area (H1) is probably related to H1 in the first layer, but it shifts to the southeast slightly. Another higher velocity area (H2) is just beneath the low velocity (L1) in the first layer. It should be noted that many earthquakes occur in high velocity areas, particularly near H2. A low velocity area (L1) is found in the southern part where earthquakes are totally absent.

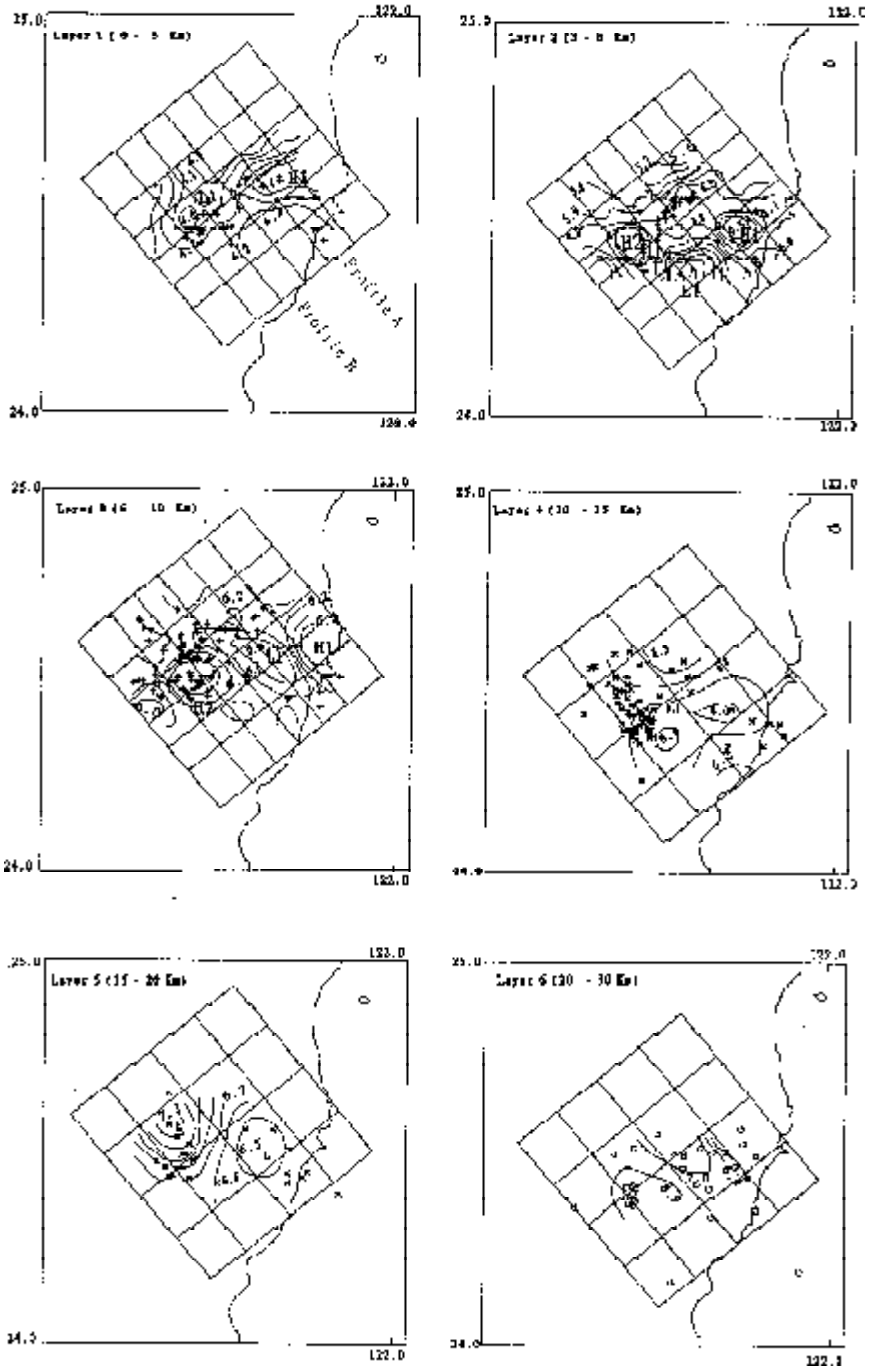

Figure 3. P-wave velocity structures are presented by contours in the areas where the inverted resolution is greater than 0.5. Values marked along the contours are P-wave velocity (km/sec). Earthquakes with different depths are also plotted with different markers: plus (0-10 km), cross (10-20 km) and circles (20-30 km).

In the third layer (6-10 km), the general trend of the velocity structures is significantly different from those in the upper two layers. Unlike the trending in the NE-SW direction in the upper two layers, the general trend of the velocity structures is along the NW-SE direction in the third layer. Two higher velocity areas (H1 and H2) are also found in the eastern and western parts in the study area, respectively. Compared with the higher velocity regions in the second layer, both high velocity areas in this layer shift to the east and become larger. Again, most earthquakes are located in the high velocity area (H1). There is a lower velocity region (L1) between the two higher velocity regions.

In the deeper layers, lateral variation in the velocity structures becomes simple. This might depend on whether the raypath density is too sparse to invert detailed structures or lateral variations really become simple. Regardless, velocities in the eastern part of the study area are generally lower than those in the western part in the fourth (10-15 km) and fifth (15-20 km) layers. In addition, only a few earthquakes are located in the lower velocities. In the sixth layer (20-30 km), high velocities are found in the central part of the study area.

RELOCATED SEISMICITY

A total of 257 earthquakes are relocated using the three-dimensional velocity model (Fig. 4). Improvement in the average quality of the relocated earthquakes can be seen from the statistical comparison of the root-mean-square (RMS) and errors in the horizontal and vertical components (ERHZ) between the original and the relocated earthquakes (Fig. 5). The RMS and ERHZ of the earthquakes relocated using the three-dimensional model are better than those before the relocation and those from the one-dimensional model.

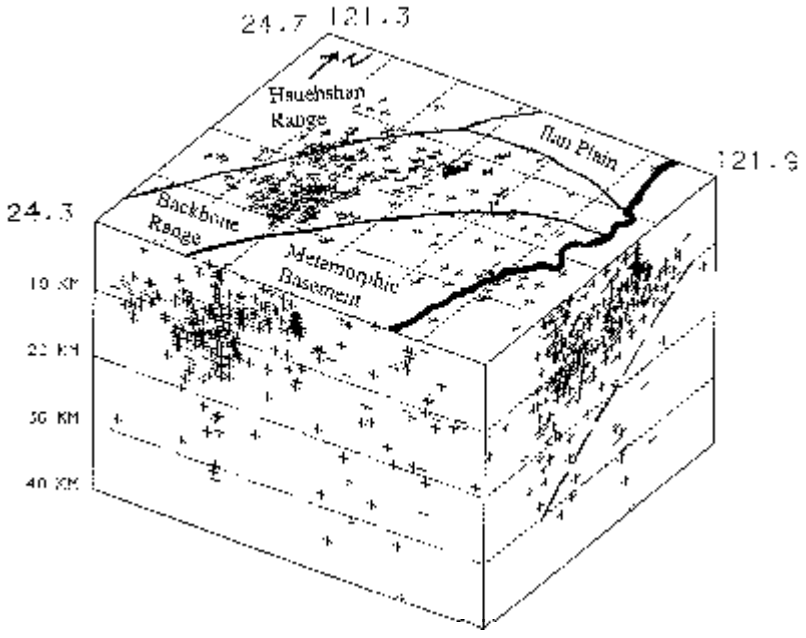

Figure 4. Projections of 257 earthquakes (+) relocated using the three-dimensional model.

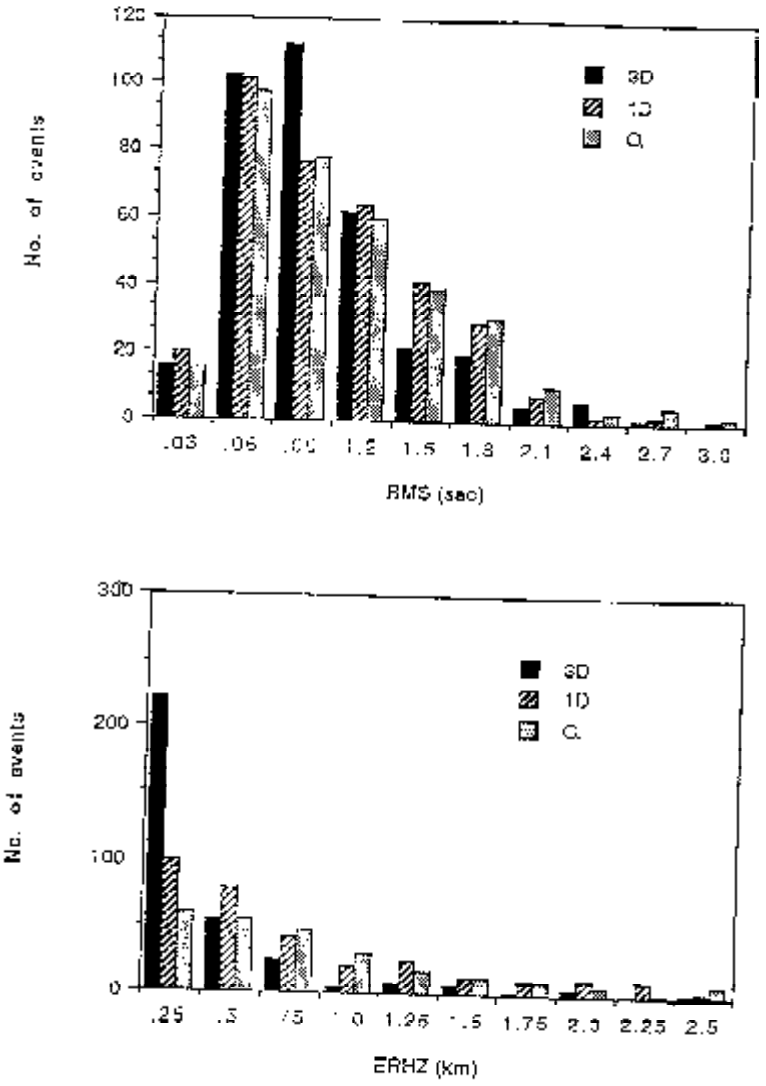

Figure 5. Statistical comparisons of (a) RMS and (b) ERHZ between the original and the relocated earthquakes.

Most of the relocated earthquakes (Fig. 4) are limited between the Neodow and Wumaoshan faults, particularly around Tuchang. Many of the focal depths of these earthquakes are less than 20 km. Projection of hypocenters on the north-south profile shows the thickness of this seismic zone increases toward the south, from 10 km to 20 km (schematized by a dashed

line in Figure 4). In other words, shallower earthquakes are located in the northeast portion near the Ilan plain, while deeper ones are located in the southwestern portion. A similar feature can also be roughly seen from the hypocenter projection on the east-west profile.

DISCUSSION

In order to describe the lateral variations in velocity structures and seismicity in more detail, velocity perturbations of the P-waves are plotted along two profiles that are perpendicular to the strike of the main structures. These profiles include the Chingshui and Tuchang geothermal area.

In Profile A (Fig. 6a) which cuts through the Chingshui area, the perturbation of the P-waves near the surface (0- 3 km in depth) increases significantly toward the southeast between the Neodou and Wumaushan faults. The most negative perturbation (L1 with -14%) is found in a shallow region of the NW portion around the Neodou fault, which merges toward the northeast beneath the Ilan plain (Tseng, 1977). This negative perturbation, extending to the depth of 6 km, probably reflects the western extension of the Ilan plain. On the other hand, the most positive perturbations in the uppermost crust are located in two areas: the one with +10% perturbation (H1) is around the Wumaushan fault at the depths of 0-3 km and the other with +9% perturbation (H2) is beneath the Tanao formation at the depths of 3-6 km. The general pattern of velocity perturbations in the mid-crust is opposite to that in the uppermost crust. In the northwestern portion, a +5% positive perturbation (H3) occupying the depths of 10-15 km is just the negative perturbation of L1. In the southeastern portion, a -4.5% negative perturbation (L2) is found at depths of 6-15 km just beneath the positive perturbations (H1 and H2).

In Profile B (Fig. 6b), which cuts through the Tuchang area, velocity perturbations do not vary significantly near the surface, except for a major negative perturbation (L1 with -5%) in the middle of the profile around the Hanchi and Hsiaonanao faults. The Tuchang geothermal area is near the Hsiaonanao fault. East of the Wumaoshan fault, velocity perturbations are negative and the most negative perturbation (L2 with -9%) is located at the depth of 3-6 km. On the other hand, the most positive perturbation in this profile is located at depth between 15-20 km just beneath the Tuchang geothermal region.

CONCLUSIONS

One-dimensional models of both P- and S-wave velocities show that a major discontinuity in the upper crust is at the depth of 3 km in the Chingshui-Tuchang geothermal area. A significantly low S-wave velocity layer at depths between 10-15 km in the mid-crust is likely to indicate existence of a partially molten magma. Three-dimensional velocity structures show that the lateral variations of P-wave velocity in the shallow depths are generally associated with the geological structures near the surface and that lower velocities are found in the major geothermal areas. Relocated earthquakes using the three-dimensional model show that most earthquakes are located in high velocity areas within the upper crust. Shallower earthquakes are located in the northeast portion near the Ilan plain, while deeper ones in the southwestern portion of the study area.

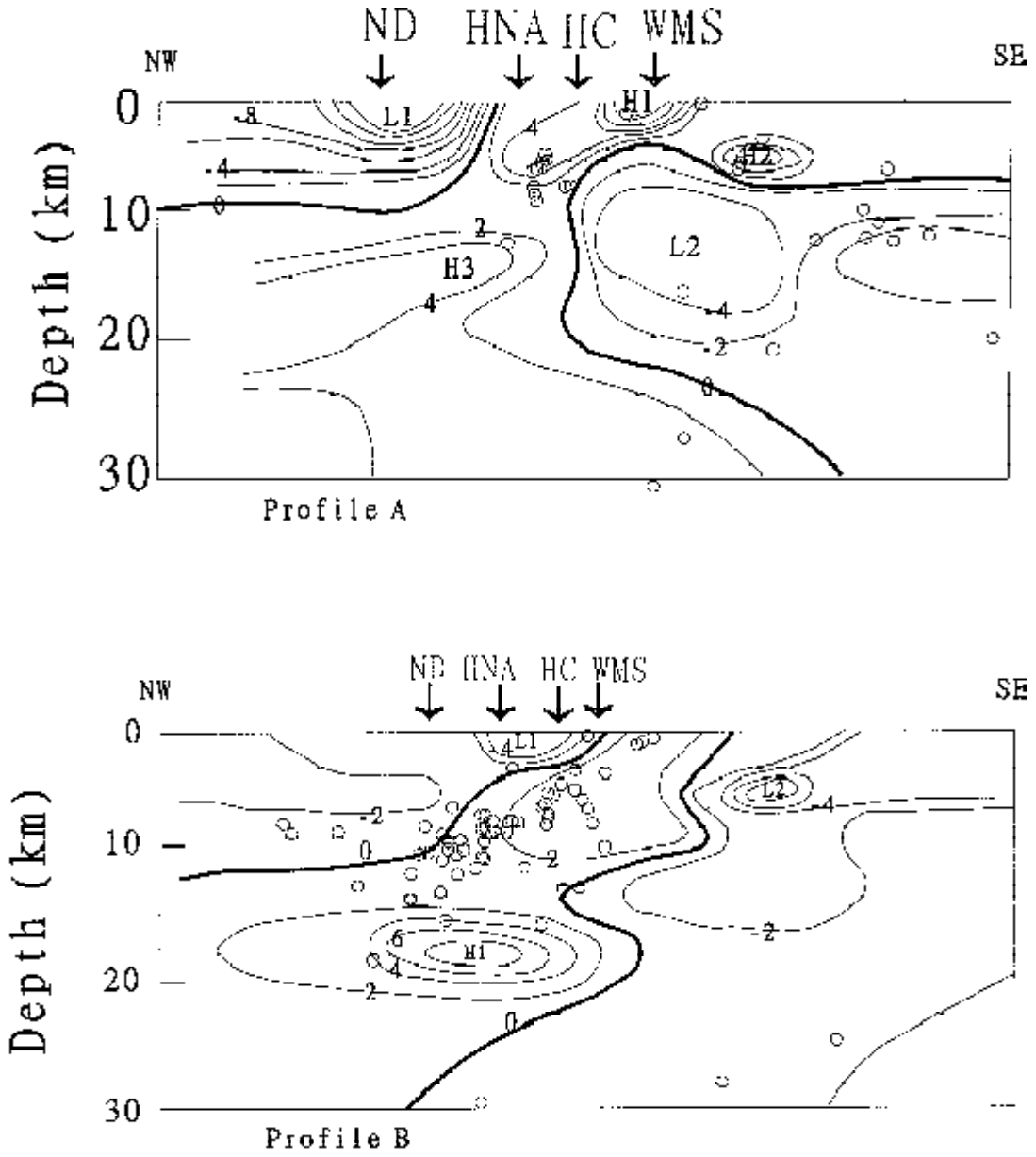

Figure 6. Perturbations of the P-wave velocity along two profiles in the NW-SE direction. Profile A cuts through the Chingshui geothermal area, while Profile B cuts through the Tuchang geothermal area. The locations of the Neodou fault, Hsiaonanao fault, Hanchi fault and Wumaoshan fault are marked by ND, HNA, HC, and WMS, respectively, at the top of both profiles.

ACKNOWLEDGMENTS

The authors would like to thank Prof. C. S. Wang for his constructive review, Prof. S. B. Yu for his kind assistance in collecting the seismic data and Prof. S. W. Roecker for provided inversion programs. This is also a contribution of the Institute of Earth Sciences, Academia Sinica, Taiwan, ROC.

REFERENCES

Chatterjee, S.N., Pitt, A.M., and Iyer, H.M. (1985) Vp/Vs ratios in the Yellowstone national part region Wyoming: *J. Volcanol. Geotherm. Res.*, **90**, 10223-10236.

Ho, C.S. (1986) An introduction to the geology of Taiwan, explanatory text of the geological map of Taiwan: *The Ministry of Economic Affairs*, Taipei, Taiwan, 153p.

Lin, C.H., Yeh, Y.H, and Roecker, S.W. (1989) Seismic velocity structures beneath the Sanyi-Fengyuan area, central Taiwan: *Proc. Geol. Soc. China*, **32(1)**, 101-120.

Liu, C.C. (1995) The Ilan plain and the southwestward extending Okinawa trough: *J. of Geol. Soc. China*, **38(3)**, 229-242.

Majer, E.L. and McEvilly, T.V. (1979) Seismological investigations at The Geysers geothermal field: *Geophysics*, **44**, 246-269.

Roecker, S.W. (1982) The velocity structure of the Pamir-Hindu Kush region: possible evidence of subduct crust: *J. Geophys. Res.*, **90**, 7771-7794.

Roecker, S.W., Yeh, Y.H., and Tsai, Y.B. (1987) Three-dimensional P and S wave velocity structures beneath Taiwan: deep structure of an arc-continent collision: *J. Geophys. Res.*, **92**, 10547-10570.

Suppe, J. (1984) Kinematics of arc-continent collision, flipping of subduction, and back-arc spreading near Taiwan: *Mem. Geol. Soc. China*, **6**, 21-33.

Tsai, Y.B., Yu, S.B., and Liaw, H.B. (1978) Microearthquake activity in two geothermal areas of Taiwan: National Science Council Monthly, 6(2), 102-115.

Tseng, C.S. (1977) Geology and geothermal occurrence of the Chingshui and Tuchang districts, Ilan: *Petro. Geol. of Taiwan*, **15**, 11-23.

Yeh, Y.H., Lin, C. H. and Roecker, S.W. (1989) A study of upper crustal structures beneath northeastern Taiwan: possible evidence of the western extension of Okinawa trough: *Proc. Geol. Soc. China*, **32 (2)**, 139-156.

Yu, S.B., Liu, W.H., Tsai, Y.B. (1977) A study of microearthquakes of the Chingshui-Tuchang geothermal area: *Inst. of Earth Sciences, Academia Sinica*, Taipei, Taiwan.